Int. J. Electrochem. Sci., 13 **(2018)** 530 – 541, doi: 10.20964/2018.01.93

International Journal of
ELECTROCHEMICAL
SCIENCE
www.electrochemsci.org

Short Communication

Anticorrosion Performance of Epoxy-Resin Coating Incorporating Talcum Powder Loaded with Sodium Tungstate

Yuanwei Liu, Yu Chen[*]

College of Chemistry & Chemical Engineering, Binzhou University, Binzhou, Shandong 256603, China
[*]E-mail: chen123yu123@163.com

Received: 18 August 2017 / *Accepted:* 27 September 2017 / *Online Published:* 1 December 2017

A self-healing coating is a smart anticorrosive coating that integrates the inhibitor-loaded talcum powder into the coating to enable long-term protection for metallic materials. In the present work, sodium tungstate was used as the corrosion inhibitor and embedded into the layered channels of talcum powder. The resulting mixture was added to an epoxy-resin coating to create a new anticorrosive and self-healing coating. The self-healing ability of the prepared coating was investigated using electrochemical impedance spectroscopy and salt spray tests. The results revealed that the arc radius increased by one order of magnitude compared to the blank samples and the impedance remained greater than 10^9 Ω cm^2 after 25 days of soaking. Meanwhile, after 90 h of salt spraying, only slight corrosion appeared at the cross-cut of the composite coating, which contained talcum powder loaded with sodium tungstate, whereas the blank samples, suffered significant corrosion. In addition, infrared analysis, XRD and scanning electron microscopy were used to study the composition and morphology of the coating.

Keywords: self-healing; epoxy-resin; sodium tungstate; inhibitor;

1. INTRODUCTION

Metallic materials are of significant importance in industry and research because of their excellent mechanical and processing properties. Unfortunately, metallic materials can be easily corroded as a result of environmental effects. Various methods have been applied to protect these materials against corrosion, such as inhibitors, organic coatings and cathodic protection [1-3]. Organic coatings are some of the most available and effective methods to protect of metal surfaces by creating a physical barrier that retard the permeation of corrosive ions or oxygen into the coatings [4]. However, because of the variations in environmental factors or mechanical properties of the coatings,

microcracks inevitably appear in the coatings during their application. When the microcracks are exposed to the atmosphere, they spread and expand, which accelerates the exfoliation and delamination of the coatings at the metal-coating interface, and decreases the service life. Currently, self-healing coatings, i.e., "smart" coatings have attracted extensive attention and emerged as a promising technique to improve the durability of organic coatings [5-8].

According to the literature [9], a smart self-healing coating can completely or partially repair damaged coated areas by releasing an inhibitor from the coating matrix in response to the internal or external stimulus. Chromate, which has excellent anticorrosion properties, has been extensively used for antirust protection of aluminum and its alloys but chromate is highly toxic and carcinogen [10]. In recent years, several environmentally friendly corrosion inhibitors have been developed, such as cerium, molybdic acid, phosphoric acid, and organic inhibitors, all of which are effective substitutes for chromate [11-13]. Nevertheless, the direct addition of inhibitors to the coating is not suitable because of their poor compatibility and solubility, which decrease the inhibitor efficiency and adhesion [14-16]. In particular, organic inhibitors can react with polymer resin, and damage the coating. Moreover, because of the interaction of the chemical bonds, it is notably difficult for the inhibitors to diffuse into the coating-metal interface to form effective protective layers [17]. Thus, the direct mixing of inhibitors into coating does not satisfy heavy-duty requirements.

To solve the incompatibility between the inhibitors and the coating matrix, two methods are commonly used: to compound the inhibitor with organic molecules such as cyclodextrin and to use a reservoir to absorb the corrosion inhibitor [18-20]. The corrosion inhibitor can be loaded in the reservoir and released as a response to external stimuli, to self-heal the coatings [21-26]. The main external stimuli are the pH level, ionic strength, temperature, ultrasonic treatment, and alternating electric and magnetic fields. Recently, researchers have developed inorganic compounds where ion exchange occurs [27-30].

The ions of corrosion inhibitors can be introduced into the interlayer or pores of the materials, where the corrosion inhibitor can be stored. Using inorganic compounds as fillers in the anticorrosion coatings, we can prevent various problems such as poor compatibility and inefficient corrosion inhibition (induced by direct contact between the corrosion inhibitor and the polymer) [31,32]. When the corrosive ions penetrate the coating, the ion exchange between the ion-exchange filler and the intrusive ions occurs, and ions from the corrosion inhibitor are released to protect the metallic matrix. However, the application of these inorganic ion-exchange fillers only suppresses the cathodic reaction at the interface between the filler and the metal. Thus, a comparable corrosion inhibition to that obtained with chromate is not achieved.

Despite all these problems, the method of in situ intercalation and adsorption with nanosilicates produces a notably effective composite [33]. The in situ intercalation and adsorption process refers to intercalating the corrosion inhibitor into the interlayers of the layered nanosilicate material to store the corrosion inhibitor. The channels in the layered nanomaterial offer layered blocking and restriction and can extend the diffusion path of the corrosive media and O_2. Consequently, the coatings can be made less permeable. In addition, because layered nanosilicates are self-suspendable and easily dispersible in coatings, the incompatibility between the corrosion inhibitor and the coatings is improved.

In the present work, an efficient economical self-healing coating was prepared from epoxy coating implanted with talcum powder loaded with sodium tungstate as corrosion inhibitor using the in situ intercalation and adsorption method. The anticorrosion properties and self-healing mechanism were systematically investigated with electrochemical impedance spectroscopy (EIS), salt spraying, FTIR, XRD and SEM.

2. EXPERIMENTAL

2.1 Incorporation of corrosion inhibitor

Talcum powder ($Mg_3(Si_4O_{10})(OH)_2$)) was loaded with inhibitor sodium tungstate ($Na_2WO_4.2H_2O$) using the intercalation and adsorption method. Briefly, 2 g analytical reagent grade talcum powder (Sinopharm Chemical Reagent Co.Ltd) was added to a certain concentration (5 g/L) of sodium tungstate (Sinopharm Chemical Reagent Co.Ltd); then the mixed solution was taken into a water bath of vibration at 25±1 °C for 2 h. After suction filtration, the residue was vacuum dried at 70±1 °C for 12 h to complete the reservoir of talcum powder and sodium tungstate (LSi inhibitor), which is called the intercalated sample in this manuscript.

2.2 Substrate preparation

Tinplate samples of size 125 mm × 50 mm × 1 mm were polished using abrasive papers with different degrees of roughness (240 #, 400 #, and 1000 #); then the dust and fragments were removed from the tinplate surface. After the tinplate samples were washed with acetone and double distilled water, they were immersed into a KH570 ethanol solution (6%) for 1 h of hydrolysis. Finally, the tinplate samples were dried at 90±1 °C for 1 h.

2.3 Preparation of composite coatings

First, the prepared reservoir (1.5913 g) was added to 15 mL tetraethylenepentamine solution (curing agent). After 12 h of magnetic stirring, 26.0657 g epoxy resin was added. The mixed solution was stirred for another 5 h to yield a well-mixed LSi-inhibitor–epoxy coating. Finally, the coating was deposited on the processed tinplate samples; the ensemble was held at 25±1 °C for 2 d and dried in an oven at 80±1 °C.

2.4 Characterization of intercalated structure of corrosion-inhibitor reservoir

Fourier transform infrared spectroscopy A sample of the coatings was mixed with a trace amount of potassium bromide (KBr) powder, ground, and compressed into tablets. Then, Fourier

Transform Infrared Spectroscopy (FTIR) of 500 cm^{-1} and 4000 cm^{-1} was conducted using a Nexus 470 (Nicolet) FT-IR spectrometer.

X-ray diffraction analysis The composition of the prepared samples were identified by glancing angle X-ray diffraction (XRD) which was conducted with a RIGAKU D/MAX 2550 diffractometer using Cu *K*a radiation (λ = 0.154056 nm) at a scan rate of 5 °/ min, and the tube source was operated at 40 kV and 250 mA.

Scanning electron microscopy The morphology of the samples was recorded using scanning electron microscopy (s-480, Hitachi Corporation, Japan) with an acceleration voltage of 15 kV.

2.5 Electrochemical impedance spectroscopy

Electrochemical tests were performed with a traditional three-electrode system where tinplate samples with different composite coatings served as the working electrode, the saturated calomel electrode (SCE) and platinum (Pt) electrode were used as the reference and auxiliary electrode, respectively. The electrolyte solution of a 3.5 wt.% NaCl solution was prepared from analytical grade chemical and double distilled water. Electrochemical polarization studies were performed using an electrochemical workstation (CHI660A, China) at a scan rate of 1 mV/s. The electrochemical impedance was measured on the tinplate electrodes that were soaked for different time periods using an impedance measurement unit (PARSTAT 2273, Advanced Electrochemical System) in a frequency range of 100 KHz - 0.01 Hz with an amplitude of 5 mV at the open circuit potential. The EIS data were analyzed with the Z-view software.

2.6 Salt spray tests

Salt-spray experiments were conducted using the rectangular tinplate specimens. Long scratches were made with a sharp tool, to accelerate the corrosion process in a salt spray chamber. The chamber was maintained at 35±1 °C using 5.0 wt.% NaCl solution.

3. RESULTS AND DISCUSSION

3.1 Structure characterization

Fig.1 shows the FTIR curve of talcum-powder and the intercalated sample (talcum-powder loaded with 5 g/L sodium tungstate). The intercalated sample exhibited the typical infrared-absorption characteristics of talcum-powder compounds. For the talcum-powder sample, a strong and wide absorption band at 3200 - 3600 cm^{-1} appears as shown in Fig.1a, which corresponds to the contraction of the hydrogen bond of hydroxyl on the layer and to the interlayer crystalline water [34,35]. Furthermore, for the intercalated sample, a new peak related to the absorption feature, which was induced by the expansion and vibration of the bridge bond W–O–W appears at 860 cm^{-1}, which

suggests the presence of tungstate ions [36]. Thus, sodium tungstate was successfully intercalated into the talcum powder.

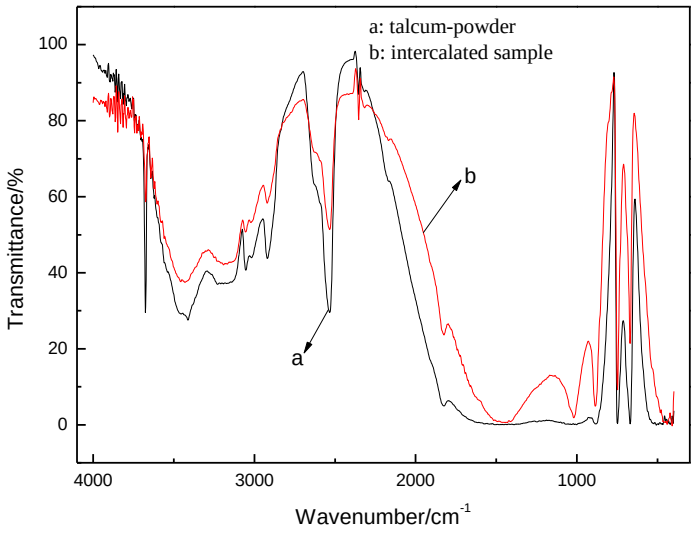

Figure 1. FTIR curve of (a) talcum powder; (b) intercalated sample (talcum powder loaded with 5 g/L Sodium tungstate).

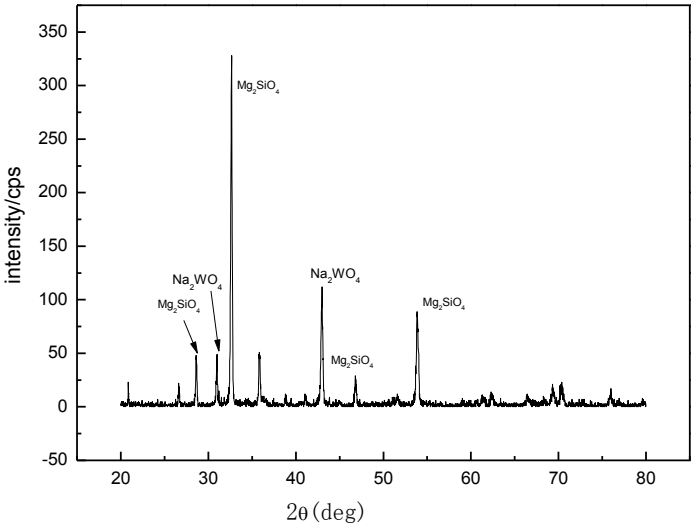

Figure 2. X-rays diffraction patterns of the intercalated sample (talcum powder loaded with 5 g/L sodium tungstate).

The XRD patterns of the intercalated sample are shown in Fig.2. The characteristic peaks appeared at 32.425° 2θ and 43.065° 2θ which indicates the presence of sodium tungstate [37,38] and further proves the successful intercalation of sodium tungstate into talcum powder. Fig.3 shows the surface morphology of the composite coatings after they are soaked in a corrosive NaCl solution (3.5 wt.%) for 1 d and 7 d. In Fig.3a, cracks obviously appeared on the composite coating, which suggests that the corrosive chemicals (mainly H_2O, O_2 and Cl^-) permeated the coating. When the immersion

time increased to 7 days, some linear coverings with a regular arrangement appeared on the coating surface, with no obvious cracks, as shown in Fig.3b. Thus, the corrosion-inhibitive ions of WO_4^{2-} are are released by the composite coatings, accomplishing the self-healing process.

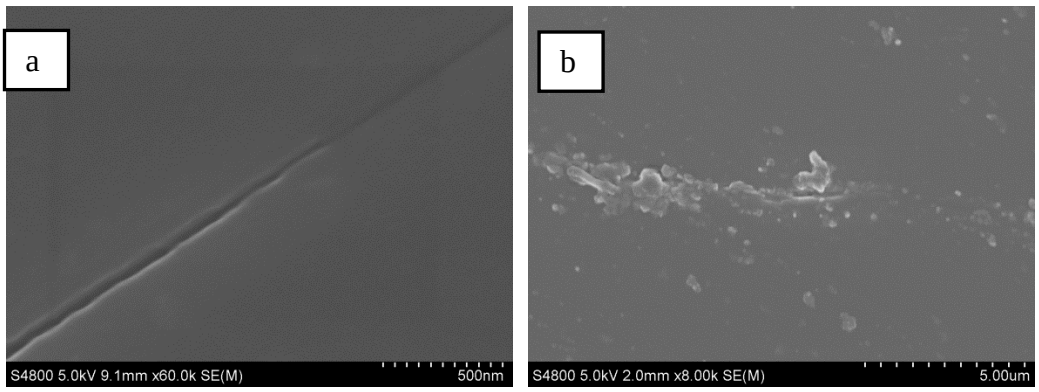

Figure 3. SEM of the coatings modified with talcum powder loaded with 5 g/L Sodium tungstate after (a) one day; (b) 7 days immersion time in 3.5 wt.% NaCl solution.

3.2 Potentiodynamic polarization measurement

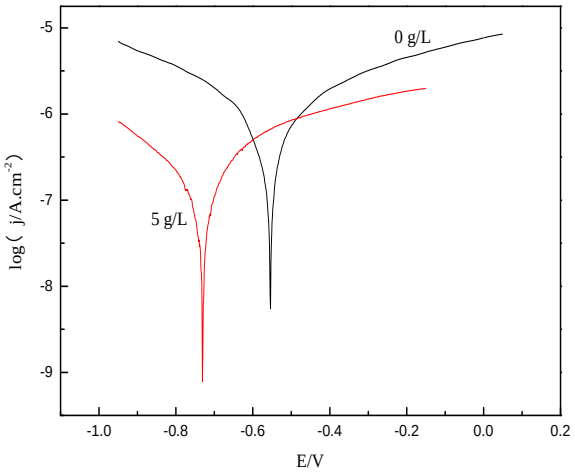

Figure 4. Polarization curves of coatings modified with talcum powder loaded with 5 g/L sodium tungstate after 7 days immersion in 3.5 wt.% NaCl solution.

The polarization curves of the coatings modified with talcum powder, which was loaded with 5 g/L sodium tungstate after 7 days of immersion in a 3.5 wt.% NaCl solution are presented in Fig.4. It is obvious that the corrosion potential moves in the negative direction, and both anodic and cathodic reactions are retarded after the addition of talcum powder with 5 g/L sodium tungstate into coating. Meanwhile, neither the anodic nor the cathodic slope of the potentiodynamic polarization curves changed in the absence and presence of talcum powder loaded with 5 g/L sodium tungstate; thus, the

corrosion mechanism is almost unchanged with the addition of talcum powder loaded with 5 g/L sodium tungstate.

The corrosion parameters (such as anodic and cathodic slopes, corrosion potential (E_{corr}), corrosion current density (I_{corr})) obtained by extrapolation of Tafel lines are listed in Table 1. It is clear that E_{corr} moved from -554 mV to -724 mV and the corrosion current density decreased from 0.921 μA/cm^2 to 0.127 μA/cm^2 with the addition of talcum powder loaded with 5 g/L sodium tungstate into the coatings, suggesting the improved protection property of the coating modified with talcum powder loaded with 5 g/L sodium tungstate.

Table 1. Electrochemical polarization parameters for the coatings modified with talcum powder loaded with 5 g/L sodium tungstate after 7 days of immersion in a 3.5 wt.% NaCl solution.

Concentration g/L	$E_{corr.}$ (mV vs. SCE)	$I_{corr.}$ (μA.cm^{-2})	B_a (mV.dec^{-1})	$-B_c$ (mV.dec^{-1})
0	-554	0.921	504	305
5	-724	0.127	482	264

3.3 Electrochemical impedance spectroscopy

The typical Nyquist diagrams (Fig.5) were recorded at the open-circuit potential of the tinplate electrodes with composite coatings in the absence and presence of talcum powder loaded with 5 g/L Sodium tungstate. The time-constant numbers of EIS plots in Fig.4 were simultaneously determined using features of the EIS diagrams (such as the number of the phase angle peak in Bode plot, number of slopes in Bode plot and number of the capacitance in Nyquist plot), and the method developed by Wit [39]. The plots show that, the EIS spectra consists of two time constants: one in the high-frequency region, which is related to the coating capacitance, and another in the intermediate-frequency region, which corresponds to the charge transfer process at the metal/coating interface [4,40].

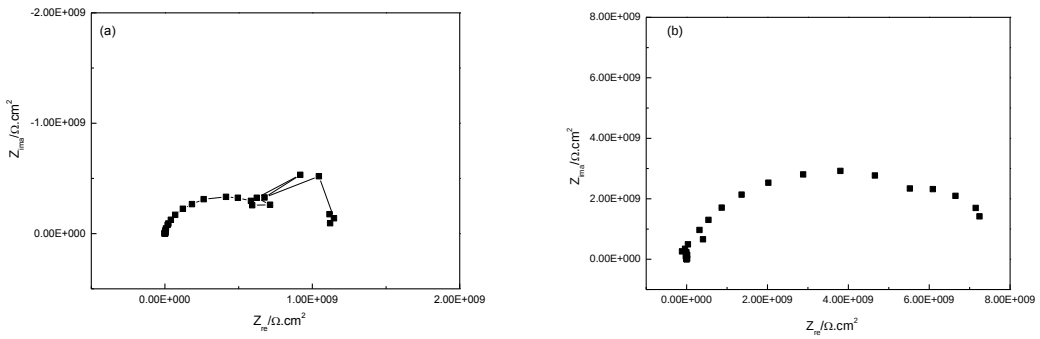

Figure 5. Typical Nyquist plots of coatings modified with (a): 0 g/L; (b) talcum powder loaded with 5 g/L Sodium tungstate after 7 days immersion in 3.5 wt.% NaCl solution.

As shown in the Nyquist plot (Fig.5a), the starting point of the semicircle almost coincides with the null point, which suggests that the solution resistance R_s decreased to approximately zero. The Nyquist plots considerably changed, as shown in Fig.5a and Fig.5b. Compared with the blank sample (0 g/L), in the high-frequency region, the samples protected by the coating with talcum powder loaded with 5 g/L sodium tungstate have a larger-diameter semicircular impedance arc, which indicates that after talcum powder loaded with 5 g/L sodium tungstate was added into the composite coating, the anticorrosion property of the samples improved. Fig.5b shows that the impedance of the samples treated with talcum powder loaded with 5 g/L sodium tungstate is approximately one order of magnitude greater than that of the blank samples. Thus, the coating processed by 5 g/L sodium tungstate significantly enhances the corrosion resistance of the metal matrix in extreme environments, which blocks the effect of corrosive media. This result is mainly attributed to the strong impedance of sodium tungstate, which exchanges ions with the corrosive particles, and intercepts the charge transfer of corrosive anions. Accordingly, the diffusion coefficient of the corrosive anions decreases. Moreover, sodium tungstate adsorbs on the surface of the metal matrix, which creates a recovery effect and contributes to the improved corrosion resistance of composite coatings.

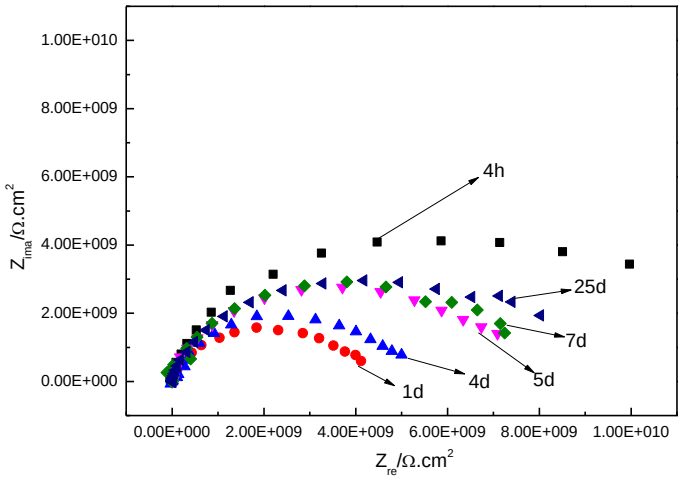

Figure 6. EIS for the coating modified with talcum powder loaded with 5 g/L sodium tungstate after different immersion time in the 3.5 wt.% NaCl solution.

Fig.6 shows the EIS results for the composite coating with a 5 g/L talcum powder loaded with sodium tungstate concentration at different immersion time. The EIS spectra obviously consist of two time constants. The depressed semi-circle with centers below the real axis, which is known as the "frequency dispersion", is related to the roughness and heterogeneity of the coating and electrode surface and suggestes the replacement of the capacity by a constant phase element (CPE) [41]. The reason may be the heterogeneity of the water uptake phenomenon [42,43]. The impedance of the constant phase element is described as follows [44-46]:

$$Z_{CPE} = \frac{1}{Y_0 (j\omega)^n} \qquad (1)$$

where Y_0 is the magnitude of the CPE, j is the square root of -1, ω is the angular frequency, and n is the phase shift which is related to the surface inhomogeneity whose value lies between 0 and 1. The general unit for CPE is F cm^{-2}.

The corresponding equivalent electrical circuit (EEC) [40] in Fig.7 is used to fit the EIS data with the Z-view software and the fitted results are listed in Table 2. This equivalent circuit has been used to describe the behavior of galvanized steel coated with a model epoxy [47]. The elements in the EEC are as follows: R_s is the solution resistance, CPE_c is the coating capacitance, R_{po} represents the resistance in the pores of the coating, CPE_{dl} is the double-layer capacitance of the solution below the coating and metal matrix, R_{ct} is the charge-transfer resistance produced in the electrochemical dissolution reaction below the coating.

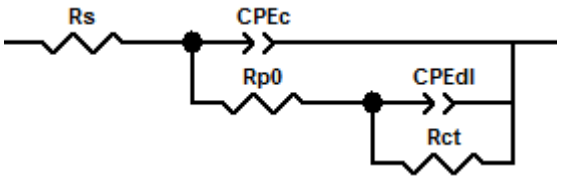

Figure 7. EEC used for simulating the impedance spectra.

Table 2. Electrochemical parameters for the composite coating modified with 5 g/L Sodium tungstate at different immersion time.

Time (h)	R_{po} ($\Omega \cdot cm^2$)	R_{ct} ($\Omega \cdot cm^2$)	Q_c ($F \cdot cm^{-2}$)	n_c	Q_{dl} ($F \cdot cm^{-2}$)	n_{dl}	$R_{po}+R_{ct}$ ($\Omega \cdot cm^2$)
4	8.07E5	8.86E9	2.49E-10	0.911	6.95E-11	0.971	8.86E9
24	9.67E5	4.16E9	5.90E-11	1.00	2.35E-10	0.816	4.16E9
96	3.02E8	4.05E9	5.94E-11	1.00	1.50E-10	0.902	4.35E9
120	6.65E6	7.16E9	4.64E-11	1.00	1.57E-10	0.798	7.17E9
168	1.76E7	7.02E9	1.38E-10	0.819	4.29E-11	1.00	7.04E9
600	6.87E6	7.93E9	8.73E-11	0.978	8.72E-11	0.623	7.94E9

With the increase in soaking time, the impedance (R_{po}+R_{ct}) of the sample protected by the intercalated composite coating with talcum powder first decreases and subsequently increases, according to the fitted results in Table 2. During the initial stage of soaking, water, O_2 and other corrosive ions (Cl^-) may gradually infiltrate the coating matrix, weaken its physical shielding capacity and decrease the impedance [48]. After one day of soaking, the sodium tungstate between the layers of talcum powder constantly exchange ions with Cl^- anions. However, the corrosive Cl^- anions can be intercepted and fixed, which contributes to the decrease in Cl^- concentration in the metal matrix and reduce the corrosion at the metal surface. Meanwhile, the sodium tungstate is continually released and subsequently adsorbed onto the metal matrix. In the present work, the accumulated sodium tungstate

covers the corroded area, which can explain the recovery and corrosion-inhibition effects. Meanwhile, the impedance of the coating remains greater than 10^9 Ω cm^2 after 25 days of soaking, which indicates an effective protection of the metal matrix from 3.5 wt.% NaCl solution.

3.4 Salt-spray test

Figure 8. Corrosion morphology of coating after 90 hours of neutral salt spraying: (a) without; (b) with talcum powder loaded with 5 g/L sodium tungstate.

The salt-spray corrosion resistance of the samples without and with the talcum powder loaded with 5 g/L sodium tungstate was investigated by making long scratches on the sample surface. Fig.8 shows the morphology of the samples after 90 hours of neutral salt spraying. The results reveal slight corrosion in the cross-type cut for the sample with sodium-tungstate-loaded talcum powder, whereas severe pitting appeares in the cross cut of the control sample and the matrix was severely corroded. This result indicates that the sample protected by the organic coating with sodium tungstate has good resistance to corrosion. The primary reason for this result is that, through ion exchange, sodium tungstate adsorbs onto the surface of the metal matrix, shields the matrix and inhibits the corrosion process. Meanwhile, Cl^- ions exchange with sodium tungstate and are fixed among the layers of talcum powder, which reduces the concentration of corrosive ions that permeated onto the matrix surface. Consequently, the resistance to chemical media and salt spray is improved.

4. CONCLUSION

In this paper, sodium tungstate was used as a inhibitor between the layers of talcum powder using the intercalation and adsorption method which was dispersed into epoxy resin as an additive. The

resulting mixture was coated onto the surface of the tinplate, formed a new composite epoxy anticorrosive coating. The EIS results show that the corrosion resistance of the tinplate significantly increases because of the above additions into the epoxy coating and the impedance of the coating remains greater than 10^9 Ω cm^2 after 25 days of soaking, which demonstrates that the composite epoxy anticorrosive coating, which is prepared by intercalation and adsorption protects the metal matrix from corrosion, even in extremely corrosive environment. The ion exchange between sodium tungstate and corrosive anions fixes the corrosive anions to a certain degree, which extends the path of the corrosive media that pass through the coating matrix. Thus, the composite coating provides higher resistance to corrosion.

ACKNOWLEDGEMENTS
The authors wish to acknowledge the financial supports of the National Natural Science Foundation of China (Project 21403194), the Scientific Research Award Foundation for Shandong Provincial (ZR2014EMQ007) and the Doctoral Research Foundation of Binzhou University (2017Y01).

References

1. J. Carmona, P. Garcés and M.A. Climent, *Corros. Sci*. 96 (2015) 102.
2. P. Refait, M. Jeannin, R. Sabot, H. Antony and S. Pineau, *Corros. Sci*. 90 (2015) 375.
3. A.M. Atta, G.A. El-Mahdy, H.S. Ismail and H.A. Al-Lohedan, *Int. J. Electrochem. Sci*., 7 (2012) 11834.
4. M.F. Montemor, D.V. Snihirova, M.G. Taryba, S.V. Lamaka, I.A. Karsonakis, A.C. Balaskas, G.C. Kordas, J. Tedim, A. Kuznetsova, M.L. Zheludkevich and M.G.S. Ferreira, *Electrochim. Acta* 60 (2012) 31.
5. A. Kumar, L.D. Stephenso and J.N. Murray, *Prog. Org. Coat*. 55 (2006) 244.
6. A.S. Hamdy, I. Doench and H. Möhwald, *Electrochim. Acta* 56 (2011) 2493.
7. J. Carneiro, J. Tedim, S.C.M. Fernandes, C.S.R. Freire, A.J.D. Silvestre, A. Gandini, M.G.S. Ferreira and M.L. Zheludkevich, *Prog. Org. Coat*. 75 (2012) 8.
8. H.D. Johansen, C.M.A. Brett and A.J. Motheo, *Corros. Sci*. 63 (2012) 342.
9. F. Cotting and I.V. Aoki, *Surf. Coat. Technol*. 303 (2016) 310.
10. M. Kendig, S. Jeanjaquet, R. Addison and J. Waldrop, *Surf. Coat. Technol*. 140 (2001) 58.
11. J. Carneiro, J. Tedim, S.C.M. Fernandes, A. Gandini, M.G.S. Ferreira and M.L. Zheludkevich, *Surf. Coat. Technol*. 226 (2013) 51.
12. M.L Zheludkevich, R. Serra, M.F. Montemor, K.A. Yasakau, I.M.M. Salvado and M.G.S. Ferreira *Electrochim. Acta* 51 (2005) 208.
13. J. Sinko, *Prog. Org. Coat*. 42 (2001) 267.
14. N.N. Voevodin, N.T. Grebash, W.S. Soto, F.E. Arnold and M.S. Donley, *Surf. Coat. Technol*. 140 (2001) 24.
15. D.G. Shchukin, M. Zheludkevich, K. Yasakau, S. Lamaka, M.G.S. Ferreira and H. Möhwald, *Adv. Mater*. 18 (2006) 1672.
16. K.A. Yasakau, M.L. Zheludkevich, O.V. Karavai and M.G.S. Ferreira, *Prog. Org. Coat*. 63 (2008) 352.
17. D. Snihirova, S.V. Lamaka, M. Taryba, A.N. Salak, S. Kallip, M.L. Zheludkevich, M.G.S. Ferreira and M.F. Montemor, *ACS Appl. Mater. Interfaces*, 2 (2010) 3011.
18. R.S. Jadha, D. G. Hundiwale and P.P. Mahulika, *J Appl Polym Sci*. 119 (2011) 2911.
19. M. Samadzadeh, S.H. Boura, M. Peikari, A. Ashrafi and M. Kasiriha, *Prog. Org. Coat*. 70 (2011) 383.

20. V.S. Moynot,S. Gonzalez and J. Kittel, *Prog. Org. Coat*. 63 (2008) 307.
21. A. Chenan, S. Ramya, R.P. George and U.K. Mudali, *Ceram. Int*. 40 (2014) 10457.
22. E. Roussi, A. Tsetsekou, A. Skarmoutsou, C.A. Charitidis and A. Karantonis, *Surf. Coat. Technol*. 232 (2013) 131.
23. A. Yabuki, A. Kawashima and I.W. Fathona, *Corros. Sci*. 85 (2014) 141.
24. K.J. Jothi and K. Palanivelu, *Appl. Surf. Sci*. 288 (2014) 60.
25. F. Tang, X.Y. Wang, X.J. Xu and L.D. Li, *Colloids and Surfaces A: Physicochem. Eng. Aspects*, 369 (2010) 101.
26. R.E. Newnham and G.R. Ruscha, *J. Intell. Mater. Syst. Struct*, 4 (1993) 289.
27. J.A. Syed, S.C. Tang, H.B. Lu and X.K. Meng, *Colloids and Surfaces A: Physicochem. Eng. Aspects*, 476 (2015) 48.
28. T. Siva and S. Sathiyanarayanans, *Prog. Org. Coat*. 82 (2015) 57.
29. M. Kopeć, K. Szczepanowicz, G. Mordarski, K. Podgórna, R.P. Socha, P. Nowak, P. Warszyński and T. Hack, *Prog. Org. Coat*. 84 (2015) 97.
30. M. Plawecka, D. Snihirova, B. Martins, K. Szczepanowicz, P. Warszynski and M.F. Montemor , *Electrochim. Acta* 140 (2014) 282.
31. T.T.X. Hang, T.A. Truc, T.H. Nam, V.K. Oanh, J.B. Jorcin and N. Pébère, *Surf. Coat. Technol*. 201 (2007) 7408.
32. T.A. Truc, T.T.X. Hang, V.K. Oanh, E. Dantras, C. Lacabanne, D. Oquab and N. Pébère, *Surf. Coat. Technol*. 202 (2008) 4945.
33. Y.H. Dong, L.Q. Ma and Q. Zhou, *J. Coat. Technol. Res*, 10 (2013) 909.
34. L.J. Bellamy, The Infrared Spectra of Complex Molecules, John Wiley, New York, 1954, p. 85.
35. N. Sharma, M. Deepa, P. Varshney and S.A. Agnihotry, *J. Non-Cryst. Solids*, 306 (2002) 129.
36. P.K. Varshney, N. Sharma, R. Ramachandran and S.A. Agnihotry, *Ind. J. Pure. Appl. Phys*. 37 (1999) 262.
37. G.X. Cao, X.Y. Song, H.Y. Yu, C.H. Fan, Z.L. Yin and S.X. Sun, *Mater. Res. Bull*. 41 (2006) 232.
38. Z.C. Jiang, C.J. Yu, X.P. Fang, S.B. Li and H.L. Wang, *J. Phys. Chem*. 97 (1993) 12870.
39. D.H. van der Weijde, E.P.M. van Westing and J.H.W. de Wit, *Corros. Sci.* 36 (1994) 643.
40. M. Yeganeh and M. Saremi, *Prog. Org. Coat*. 79 (2015) 25.
41. J.R. Macdonald, *J. Electroanal. Chem. Interfacial Electrochem*. 223 (1987) 25.
42. A.C. Bastos, M.G.S. Ferreira and A.M.P. Simões, *Corros. Sci*. 69 (2013) 87.
43. M. Lebrini, M. Lagrenée, H. Vezin, M. Traisnel and F. Bentiss, *Corros. Sci*. 49 (2007) 2254.
44. I. Ahamad, R. Prasad and M. Quraishi, *Mater. Chem. Phys*. 124 (2010) 1155.
45. N.D. Nam, Q.V. Bui, M. Mathesh, M.Y.J. Tan and M. Forsyth, *Corros. Sci*. 76 (2013) 257.
46. M.H. Hussin, M.J. Kassim, N.N. Razali, N.H. Dahon and D. Nasshorudin, *Arab. J. Chem*. 9 (2016) S616.
47. M.F. Montemor, D.V. Snihirova, M.G. Taryba, S.V. Lamaka, I.A. Kartsonakis, A.C. Balaskas, G.C. Kordas, J. Tedim, A. Kuznetsova, M.L. Zheludkevich and M.G.S. Ferreira, *Electrochim. Acta* 60 (2012) 31.
48. F. Maia, K.A. Yasakau, J. Carneiro, S. Kallip, J. Tedim, T. Henriques, A. Cabral, J. Venâncio, M.L. Zheludkevich and M.G.S. Ferreira, *Chem. Eng. J.* 283 (2016) 1108.